Theory in Biosciences (2024) 143:63–77
https://doi.org/10.1007/s12064-023-00410-3

RESEARCH

Modeling stress-induced responses: plasticity in continuous state space and gradual clonal evolution

Anuraag Bukkuri[1,2]

Received: 20 July 2023 / Accepted: 13 December 2023 / Published online: 30 January 2024

Abstract

Mathematical models of cancer and bacterial evolution have generally stemmed from a gene-centric framework, assuming clonal evolution via acquisition of resistance-conferring mutations and selection of their corresponding subpopulations. More recently, the role of phenotypic plasticity has been recognized and models accounting for phenotypic switching between discrete cell states (e.g., epithelial and mesenchymal) have been developed. However, seldom do models incorporate both plasticity and mutationally driven resistance, particularly when the state space is continuous and resistance evolves in a continuous fashion. In this paper, we develop a framework to model plastic and mutational mechanisms of acquiring resistance in a continuous gradual fashion. We use this framework to examine ways in which cancer and bacterial populations can respond to stress and consider implications for therapeutic strategies. Although we primarily discuss our framework in the context of cancer and bacteria, it applies broadly to any system capable of evolving via plasticity and genetic evolution.

Keywords Eco-evolutionary dynamics · Cancer evolution · Bacterial evolution · Plasticity · Therapeutic resistance

Introduction

Therapeutic resistance is well recognized as one of the major contributors to treatment failure and poor outcomes in patients (Housman et al. 2014; Frieri et al. 2017; Vasan et al. 2019; Zaman et al. 2017). Traditionally, resistance is thought to emerge from the selection of subpopulations of cells that have acquired one or more resistance-conferring mutations (Hanahan and Weinberg 2011). However, recent studies also show the importance of phenotypic plasticity as a mechanism for mediating resistance, e.g., by cells entering a polyaneuploid, mesenchymal, inflammatory, or stem-like state (Amend et al. 2019; Chin and Lim 2019; Gonzalez et al. 2022; Katsuno et al. 2019; Li et al. 2019; Pienta et al. 2020; Pienta et al. 2021; Weng et al. 2019; Yuan et al. 2022; Zhou et al. 2020).

In order to develop novel therapeutic strategies for bacterial and cancer extinction or control, a deep understanding of their ecological (population), evolutionary (resistance), and demographic (state) dynamics is required. To this end, many mathematical models have been constructed and analyzed to elucidate various aspects of therapeutic resistance via plasticity and clonal evolution. However, most models consider only one of these mechanisms (Bukkuri and Brown 2021; Dhawan et al. 2016; Forouzannia et al. 2020; Tonekaboni et al. 2017). For the few models that incorporate both (Bukkuri et al. 2022a; Bukkuri et al. 2022b; Cunningham et al. 2021), plastic transitions are usually assumed to occur within a discrete state space.

In this paper, we use integral projection models (IPMs) to develop a method to model the ecological, evolutionary, and demographic (hereafter referred to as eco-evo-demo) dynamics of populations that evolve resistance in the face of therapy via continuous phenotypic transitions and clonal evolution. IPMs developed as an offshoot from matrix population models (Bukkuri and Brown 2023; Caswell 2001; Caswell 2012; Caswell 2019; de Vries et al. 2020) as a way to deal with population structure of a continuous nature, relaxing the requirement that organisms in a population must be classified into a set of discrete states (Easterling et al. 2000; Rees et al. 2014). These models allow ecologists and

✉ Anuraag Bukkuri
anuraag.bukkuri@moffitt.org

[1] Cancer Biology and Evolution Program and Department of Integrated Mathematical Oncology, Moffitt Cancer Center, Tampa, USA

[2] Tissue Development and Evolution Research Group, Department of Laboratory Medicine, Lund University, Lund, Sweden

demographers to understand how continuous state structure impacts a population's eco-evolutionary dynamics (Coulson 2012; Coulson et al. 2010). IPMs are typically constructed from regression models that infer how an organism's state and environment impacts its survival, growth, and reproduction (Adler et al. 2010; Dahlgren and Ehrlen 2009; Dalgleish et al. 2011; Merow et al. 2014; Nicolè et al. 2011). Such models have been used in a variety of ecological contexts, to help us understand and control invasive species (Erickson et al. 2018; Goodsman et al. 2018), the adaptation of insects and plants to climate change (Schwartz et al. 2016), herbivore–plant interactions (Hegland et al. 2010; Miller et al. 2009; Rose et al. 2005; Williams et al. 2010), optimal flowering size in plants (Hesse et al. 2008; Metcalf et al. 2003; Miller et al. 2012; Rees and Rose 2002; Williams et al. 2009), and host–parasite dynamics (Metcalf et al. 2016). We port over a more qualitative version of this framework to the cellular level and investigate the eco-evo-demo dynamics in populations subjected to environmental stress. We also investigate two facultative mechanisms by which cell populations may modulate their stress-induced responses depending on their condition in the environment: stress-induced mutagenesis (Badyaev 2005; Bjedov et al. 2003; Foster 2007; Fitzgerald et al. 2017) and facultative plasticity (Aiello et al. 2018; Amend et al. 2019; Fisher et al. 2017; Zañudo 2019; Liau et al. 2017; Pienta et al. 2020; Pienta et al. 2021; Pienta et al. 2020a; Pienta et al. 2020b; Rabé et al. 2020; Sharma et al. 2010; Shen and Clairambault 2020). Using this knowledge, we then examine the efficacy of intermittent and adaptive therapy strategies (Gatenby et al. 2009; West et al. 2020).

Methods

Analytical framework

We construct our modeling framework using IPMs. First, we outline the ecological dynamics for the most simple case in the form of an integrodifference equation:

$$n_{\bar{u},t+1}(z') = \int K_{\bar{u},t}(z,z')n_{\bar{u},t}(z)\mathrm{d}z \tag{1}$$

where n is the population distribution, u is the drug resistance trait, $z \in Z = [0,1]$ is the current state of the cell, and z' is state at the next time step. The states $z \in Z$ may represent the state of cells on epithelial to mesenchymal, adrenergic (ADRN) to mesenchymal (MES), or aneuploidy continua, for example. We assume that population density is δ peaked in u space around the mean drug resistance value, $\bar{u}$, so the ecological, demographic, and evolutionary dynamics are all dependent on solely $\bar{u}$. The kernel K can be decomposed into survival, plasticity, birth, and fecundity as follows:

$$K_{\bar{u},t}(z,z') = \underbrace{s_{\bar{u},t}(z)}_{\text{Survival}}\overbrace{G(z,z')}^{\text{Growth Kernel}} + \underbrace{b(z)}_{\text{Birth}}\overbrace{R(z,z')}^{\text{Fecundity Kernel}} \tag{2}$$

The first term is the growth kernel, often denoted by $G_{\bar{u}}(z,z')$, and the second term is the fecundity kernel, $R(z',z)$. The survival and birth functions, $s_{\bar{u},t}(z)$ and $b(z)$, are called individual components, whereas the growth and fecundity kernels, $G(z,z')$ and $R(z,z')$, are *state-redistribution components*. Under this formulation, we assume that drug resistance, u, only impacts the survival of the cells—in the future sections, we will relax this assumption. The specific forms for each of these components are

$$\begin{aligned} G(z,z') &\sim N(z,\sigma_G^2) \\ R(z,z') &\sim N(z,\sigma_R^2) \\ s_{\overline{u,t}}(z) &= \max\left(0, 1 - \mathrm{d}k - \tfrac{m(t)}{\exp(\phi z)+\beta\bar{u}}\right) \\ b(z) &= b_1\exp(b_2 z) \end{aligned} \tag{3}$$

First, consider the state-redistribution components, $G(z,z')$ and $R(z,z')$. We approximate the movement of cells through state space and the production of progeny using a Gaussian distribution. Although this is a fairly standard assumption in integral projection modeling (Easterling et al. 2000; Ellner and Rees 2006; Merow et al. 2014; Rees et al. 2014) (and indeed, G function (Bukkuri and Brown 2021; Vincent et al. 2005) and adaptive dynamics (Diekmann 2004; Kisdi and Geritz 2010) modeling), the distribution can be tailored to specific situations or fitted to data if required. In our case, the normal distribution is appropriate since cells tend to produce progeny very similar to themselves with most mutations having a small phenotypic effect. Similarly, cells tend to stay within similar cell states and only rarely drastically shift to the tail ends of their distribution.

Next, we turn our attention to the individual components. Consider the survival function, $s_{\bar{u}}(z)$. Bounded below by zero, the survival of cells is reduced by two factors. The first term, dk, captures the natural death rate and assumes a linear cost of evolvability, k. In other words, we assume that the natural death rate of a cell increases as its evolvability increases, e.g., due to mutational meltdown (Bukkuri 2022), and enforce $d > 0$ and $k \geq 0$. The second term, $\frac{m}{exp(\phi z)+\beta\bar{u}}$, captures death due the effect of drug via a Michaelis–Menten-like formulation (Bukkuri and Brown 2021; Bukkuri et al. 2022a; Bukkuri et al. 2022b), where $m(t) \geq 0$ represents drug dosage at time t, $\phi > 0$ is the impact of the cell state on survival, and $\beta > 0$ represents the impact of resistance on survival. Finally, consider the birth function, $b(z)$. The maximal birth rate of the cell is captured by b_1.

This proliferation rate is tempered by the cell's state with the multiplicative exponential term. Namely, we assume that higher cell states lead to lower birth rates (enforced by $b_2 < 0$). This survival-birth trade-off is worth stressing. Higher cell states (e.g., mesenchymal, inflammatory, or high ploidy) attain higher survival under therapy than lower cell states (e.g., epithelial, adrenergic, proliferative, or low ploidy). But this comes at a cost: a lower birth rate. This trade-off, visualized in the heatmap below (Fig. 1), is experimentally observed in a multitude of contexts across bacterial and cancer evolution (Amend et al. 2019; Chin and Lim 2019; Katsuno et al. 2019; Liau et al. 2017; Shun et al. 2019; Sánchez-Danés et al. 2018; Shen et al. 2019; Zhou et al. 2020).

From these ecological dynamics, we can then derive the evolutionary dynamics of resistance via Fisher's fundamental theorem of natural selection (Li 1967; Basener and Sanford 2018; Frank and Slatkin 1992; Lessard 1997), *sensu* the G function framework (Bukkuri and Brown 2021; Vincent et al. 2005). This approach states that evolution is the product of evolvability (the capacity to generate heritable variation upon which natural selection can act), and the selection gradient. Namely, for the discrete-time case, we have

$$\begin{aligned}\Delta\bar{u} &= \frac{k}{\bar{\lambda}}\frac{\partial\lambda}{\partial u} \\ &= \frac{k}{\bar{\lambda}}\left(\int\int \frac{\partial\lambda}{\partial K}\frac{\partial K}{\partial s}\frac{\partial s}{\partial u}\mathrm{d}z\mathrm{d}z'\right) \\ &= \frac{k}{\bar{\lambda}}\left(\int\int \mathbf{s}(\mathbf{u},\mathbf{z},\mathbf{z}')P(z,z')\frac{\beta m}{(\beta u+\exp(\phi z))^2}\mathrm{d}z\mathrm{d}z'\right)\end{aligned} \tag{4}$$

where $\bar{u}$ represents the mean drug resistance value in the population, λ is the per-capita growth rate or fitness function calculated as the spectral radius of the kernel operator (Bukkuri and Brown 2023), and $\mathbf{s}(\mathbf{u},\mathbf{z},\mathbf{z}')$ is the sensitivity of the fitness function to perturbations in the kernel operator, calculated as the normalized inner product of the reproductive and stable state distribution eigenvectors. Note that if drug resistance levels impact components other than just survival, this equation will need to be modified to incorporate the other terms via a basic application of the chain rule as shown above. Under this framework, we allow cells to respond to therapeutic stressors via both plasticity (changing cell state in a continuous and reversible fashion) and genetic evolution (evolving higher levels of resistance, u).

Numerical implementation

There are two technical points to note concerning the numerical implementation of our model. The discretized IPM kernel used in the simulations is the result of overlaying a mesh over the operator, treating it as a large finite-dimensional matrix. Thus, rather than dealing with the integrodifference equation in Equation 1 directly, we treat it as a high-dimensional, discrete-time matrix population model (Bukkuri and Brown 2023; Caswell 2001) and simply project it forward in time using matrix multiplication. The choice of mesh size (and thereby dimensionality of the resulting matrix) is a trade-off between accuracy and computational cost: The smaller the mesh size, the more accurate the numerical results, but the greater computational effort. In our case, we used a 100x100 matrix. Another aspect to consider are the boundary conditions. Since we defined a bounded interval for our state distribution, Z, we must correct for eviction, whereby individuals diffuse outside these boundaries due to the Gaussian nature of our size-redistribution kernels. To do this, we return all cells that occupy states outside Z to the boundary from which they were evicted (Merow et al. 2014) (see (Williams et al. 2012) for alternative corrections).

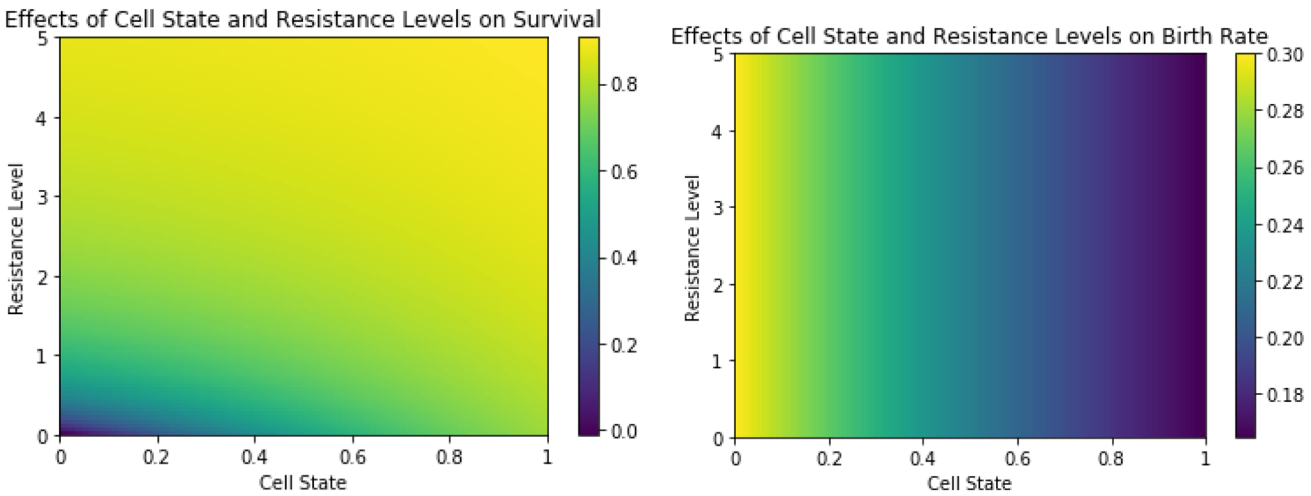

Fig. 1 Survival-Birth Trade-off: higher cell states (z) confer a greater survival under therapy but come with a lower birth rate. Assuming no cost of resistance, resistance levels (u) allow for higher survival under therapy and do not impact birth rates

Another consequence of our modeling assumptions is the existence of a small subpopulation of highly resistant cells occupying high cell states prior to drug exposure. Due to the Gaussian nature of our kernels, these cells can indeed become or generate drug-sensitive cells and vice versa. This observation has found experimental support, e.g., Shaffer et al. identify a rare population of melanoma cells that transiently display high expression of AXL in the absence of therapy. These cells are resistant to anti-BRAF therapy and have been found to stochastically give rise to drug-sensitive cells (Shaffer et al. 2017).

Results

We ran a series of simulations capturing the eco-evo-demo dynamics of populations under therapy. The parameter values used in the simulations can be found in Table 1. These parameters were chosen to be biologically plausible, numerically convenient for simulation purposes, and to clearly show differences among stress-responses and therapeutic outcomes. Although many of these parameters can quantitatively alter results (e.g., a higher birth rate and evolvability or a lower drug dosage and natural death rate can promote the survival of the cell population under therapy), the same broad qualitative trends hold.

In all simulations, the population is initialized with densities of 0.5 across all cell states for a total population size of 50 cells. This choice of initial condition is relatively arbitrary and can be customized for specific applications. Here, we assume that at time 0, the cancer is initiated as a speciation event from normal somatic cells. As such, it is far from a demographic equilibrium (Pienta et al. 2020a; Pienta et al. 2020b). Therapy will be administered as a constant dose through time once the population reaches one million cells and the simulation will be stopped once the population recovers back to the one million cell threshold or once the population size is less than 10 (an arbitrary threshold). Note that, when the cancer is detected and treatment is administered, the population has yet to reach its demographic equilibrium. This is in accordance with clinical practice and ongoing experimental studies that suggest that cancer cell populations often are not near their demographic equilibrium when treatment is given. Key summary statistics are provided in Table 2: final drug resistance level, minimum of population, time of therapeutic application, time to progression (TTP: number of time steps between the start of therapy and when the population reaches one million cells again), and time to treatment failure (TTF: number of time steps between the start of therapy and when the population starts increasing in size).

Table 1 Parameter definitions and baseline values used in simulations

Parameter	Interpretation	Value
d	Natural death rate	0.01 h^{-1}
m	Drug dosage	1 h^{-1}
ϕ	Impact of state on drug death	1.5
β	Impact of strategy on drug death	1.5
b_1	Maximal intrinsic growth rate	0.3 h^{-1}
b_2	Birth-state scaling term	−0.6
σ_R	Standard deviation of fecundity kernel	0.05
σ_G	Standard deviation of growth kernel	0.05
k	Evolvability	1
Z	State interval	[0,1]
u	Drug Resistance Level	$[0, \infty)$

Model exploration

First, we run a series of simulations to explore the dynamics of our model. We consider the following cases: baseline (parameters given in Table 1), no evolvability ($k = 0$), high evolvability ($k = 4$), low growth variance $\sigma_G = 0.01$, and high growth variance ($\sigma_G = 0.1$) (Fig. 2 and Table 2). First, note the similarities among the simulations. Since cells in lower cell states proliferate more rapidly than those in higher cell states, the average cell state in the population decreases before therapy is administered. Once the population size passes the one million cell threshold and therapy is administered, the population's demography shifts toward higher cell states, allowing the cells to minimize the effects of therapy at the cost of proliferating more slowly. This demographic transition buys time for adaptive genetic evolution to occur (Diamond and Martin 2016; Fox et al. 2019; Merilä and Hendry 2014). As resistance develops and treatment begins to fail, the population shifts toward pre-therapy demography, leading to higher proliferation rates and the eventual progression of the tumor (Table 2). However, if cells are unable to evolve resistance (i.e., $k = 0$), the population remains in a high cell state. For the parameter values chosen here, this shift in demography is not enough for the population to avoid extinction.

There are also key differences among our simulations as a result of differences in evolvability and variance. Starting with the former, note that due to the cost of evolvability, it takes more evolvable populations longer to surpass the one million cells threshold, leading to a delayed start of therapy (Table 2). Although highly evolvable populations still shift their demography to higher cell states upon administration of therapy, this demographic transition is less extreme due to the rapid evolution of resistance. Finally, as one might expect, the rapid evolution of resistance leads to a higher minimum of the population and a shorter TTP and TTF than other cases (Table 2).

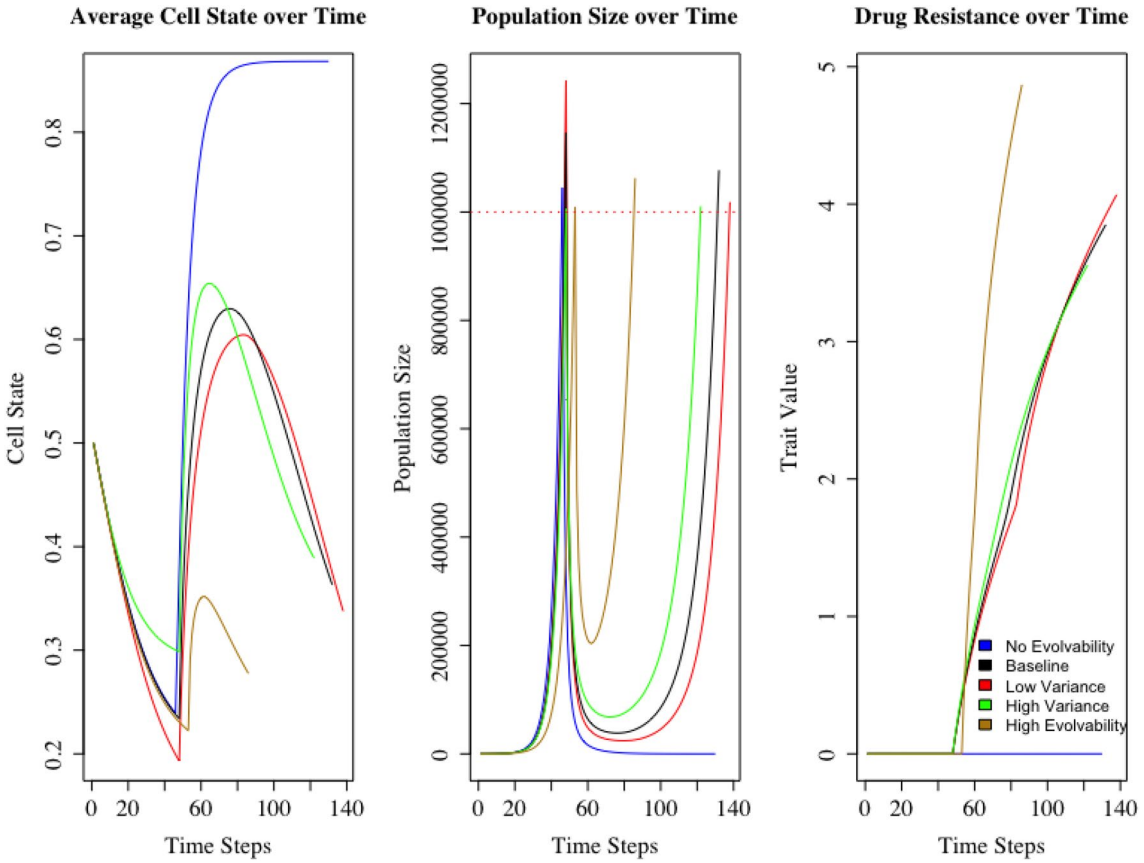

Fig. 2 Impact of evolvability and growth variance on eco-evo-demo dynamics. Blue, black, red, green, and brown lines capture dynamics of populations with no evolvability, baseline conditions, low growth variance, high growth variance, and high evolvability, respectively. Higher growth variances and evolvabilities lead to higher population minima and faster times to progression and treatment failure (color figure online)

Table 2 Model exploration summary

	Baseline	Low variance	High variance	No evolvability	High evolvability
Drug resistance	3.850	4.068	3.556	0	4.868
Minimum of population	38,443	24,375	68,137	9	203,847
Start of therapy	48	48	48	46	53
Time to progression	84	90	74	NA	33
Time to treatment failure	29	32	25	NA	10

Now, consider the impact of variance. For biological realism and simplicity, we fix the variance in the fecundity kernel and solely consider changes to the growth kernel. An increase in the variance of the fecundity kernel can be considered a form of saltational evolution (Willis 1923), *sensu* Goldschmidt's "hopeful monster" macromutations (Goldschmidt 1933) (a rather controversial theory (Dietrich 2003), particularly at the cellular level). Combining this with the fact that the fecundity kernel produces variance across states, not the resistance trait, we choose to focus solely on the impacts of variance in the growth kernel. However, due to the structure of our model, results for fecundity variance are qualitatively similar to those of growth variance, with quantitative differences arising from the magnitude of the difference between survival and birth probabilities and the interplay with evolutionary dynamics (survival is dependent on strategy but birth is not).

We see that lower variance kernels move closer to the tails of their distributions more effectively than higher variance kernels, a phenomenon that is paralleled in the pre-therapy demographic dynamics. This allows them to attain a lower average cell state and higher population size when therapy is administered. After therapy is given, the high growth variance population is able to shift its demography

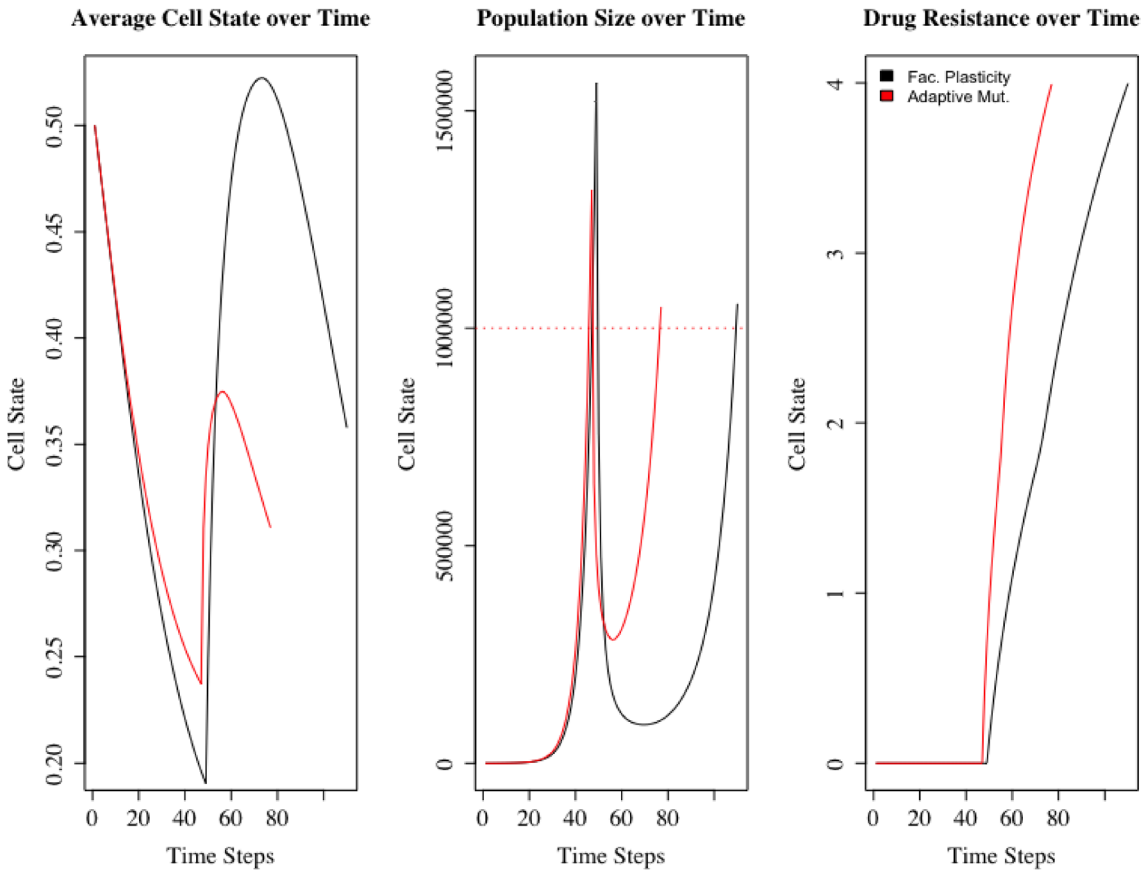

(a) Eco-evo-demo dynamics

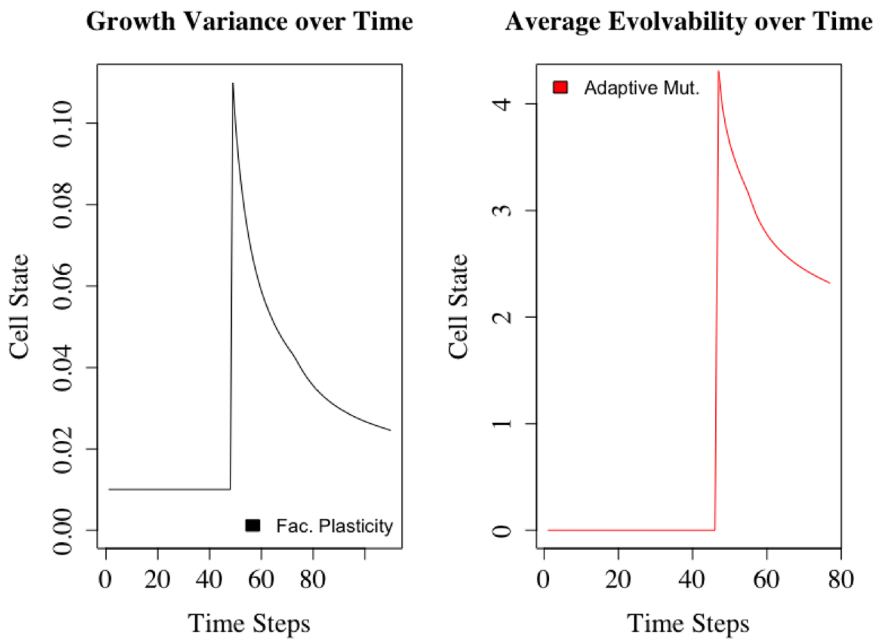

(b) Growth variance and evolvability dynamics

◂**Fig. 3** Impact of facultative stress-induced responses on eco-evo-demo dynamics. The ability of a population to modulate the extent of its plasticity or nature of its mutations in response to its condition leads to faster proliferation/higher survival pre-therapy, higher minima, and shorter times to progression and treatment failure

toward high cell states the most rapidly, reaching the highest average cell state among the evolvable populations. These factors dampen the selective pressure on the high growth variance population to evolve resistance. Thus, although this population progressed and reached treatment failure the quickest, it also evolved the least resistance (Table 2).

Facultative stress-induced responses

With a basic understanding of how variance and evolvability impact eco-evo-demo dynamics, we now examine facultative stress-induced responses that populations may undergo. Throughout this paper, we have discussed two mechanisms by which cells can adapt to a therapeutic stressor: by changing their cell state (plasticity) and by evolving higher resistance levels (genetic evolution). However, both of these adaptations come with a cost. A shift in demography toward higher cell states leads to lower proliferation rates, and a faster rate of evolution (via a high evolvability) leads to a higher death rate. Thus, it is natural to ask: What if populations could modulate their degree of plasticity and evolvability depending on their condition? In other words, what if cells could increase their plasticity and evolvability when they are stressed and decrease them when they are stable? In this section, we consider how facultative plasticity and adaptive mutagenesis impact the eco-evo-demo dynamics of populations under therapy (Fig. 3 and Table 3).

Plasticity, the process by which cells transiently adopt a distinct phenotypic identity in a non-genetic fashion, is a commonly observed stress response in cancer and bacteria. Critically, these plastic transitions are completely reversible. In bacteria, a slow-cycling drug-tolerant persister (DTP) state plays such a role, providing a stepping-stone toward more permanent genetic resistance (Sharma et al. 2010). A similar DTP state was detected in non-small cell lung cancer, melanoma, and glioblastoma (Biehs et al. 2018; Liau et al. 2017; Marion et al. 2020; Rambow et al. 2018; Sánchez-Danés et al. 2018; Shen et al. 2019). In addition, the ADRN–MES transition in neuroblastoma, epithelial-to-mesenchymal transition, and polyaneuploid transition (PAT) have all been shown to contribute to therapeutic resistance in cancer (Amend et al. 2019; Chin and Lim 2019; Katsuno et al. 2019; Shun et al. 2019; Pienta et al. 2020; Pienta et al. 2021; Weng et al. 2019; Xiaojun et al. 2022; Zhou et al. 2020). To implement facultative plasticity, we use the same parameter values as in Table 1, but let the variance in the growth kernel depend on the cell's condition: $\sigma_G = .01 + .15exp\left(-\frac{.3}{d_{drug}}\right)$ where $d_{drug} = \frac{m}{exp(\phi z)+\beta u}$ represents the drug-induced death rate for a cell in state z with resistance level u. In addition to the eco-evo-demo dynamics, we plot the change in average growth variance over time (Fig. 3).

Adaptive mutagenesis is a widely recognized phenomenon in bacterial (Bjedov et al. 2003; Foster 2007; Fitzgerald et al. 2017; Rosenberg et al. 2012), yeast (Galhardo et al. 2009; Hastings et al. 2004; Layton and Foster 2003; Lombardo et al. 2004; Lovett 2006; Petrosino et al. 2009), and (albeit to a lesser extent) cancer (Hall 1995; Finch and Goodman 1997; Rosenberg et al. 1994; Strauss 1986) evolution. Also known as stress-induced mutations, adaptive mutations describe the generation of heritable variation that occurs in response to the environment (Rosenberg 2001). To implement adaptive mutagenesis, we use the same parameters in Table 1, but let evolvability be a function of the cell's condition: $k = 5exp\left(-\frac{.1}{d_{drug}}\right)$. In addition to the eco-evo-demo dynamics, we plot the change in average evolvability over time (Fig. 3).

Before drug exposure, the variance in growth kernel and mutation rate is low. This allows the population to reach lower average cell states and proliferate more quickly or minimize natural cell death, respectively. Once therapy is applied, the population quickly increases its growth variance or evolvability. In the former case, facultative plasticity allows cells to quickly move toward higher states, whereas in the latter case, adaptive mutagenesis allows for rapid evolution of resistance. In both, the population drop is less severe (Table 3). Once the initial burst of adaptation or evolution has occurred, the population decreases its growth variance or evolvability. This allows for continued modest evolution of resistance, while allowing for higher proliferation rates or lower natural death rates. These aspects contribute to a faster rate of evolution and a shorter TTP and TTF.

Therapeutic strategies

Throughout this paper, we have seen how the potent combination of plasticity and genetic evolution allows populations to evolve and adapt to stressful conditions. This leads to the natural question: How can we develop therapeutic strategies to effectively control or drive populations to extinction given the complex interplay among ecological, evolutionary, and demographic dynamics? As done in our past work and as suggested by others, one approach is to use a life-history enlightened approach (Bukkuri et al. 2022a; Bukkuri et al. 2022b; Shen and Clairambault 2020) by attempting to block plastic transitions toward drug-resistant phenotypes. Such approaches, at the epigenetic, intracellular pathway, and microenvironmental levels, have shown promise in a variety

Table 3 Facultative plasticity and stress-induced mutagenesis results summary

	Facultative plasticity	Adaptive mutagenesis
Drug resistance	4.000	3.992
Minimum of population	87,954	283,292
Start of therapy	48	46
Time to progression	62	31
Time to treatment failure	23	11

of cancers, including glioblastoma, breast cancer, melanoma, and prostate cancer (Guler et al. 2017; Liau et al. 2017; Roswall et al. 2018; Rusan et al. 2018; Sánchez-Danés et al. 2018; Straussman et al. 2012; Wallner et al. 2006). Similarly, efforts have been made to develop drugs to target cell states that are resistant to traditional therapies (Boshuizen et al. 2018; Hangauer et al. 2017; Rambow et al. 2018; Tsoi et al. 2018; Viswanathan et al. 2017). In this section, we focus on therapeutic strategies assuming that neither of these options exist.

Specifically, we will investigate the efficacy of intermittent and adaptive therapy protocols when cells can adapt to the stressor in both plastic and genetic ways. For simplicity, we will implement therapy solely on the baseline case (see Table 1) here. Under both protocols, we let therapy begin once the population size exceeds one million cells. We focus on three statistics: minimum of population, TTF, and TTP. If extinction is the goal, the minimum of the population is the metric of most importance. If the physician is aiming at control and only has one drug, TTP is most relevant. However, if the goal is control, several drugs are available, TTF is key.

First, we begin with the intermittent therapy. Under this protocol, therapy follows a fixed administration schedule, with both treatment and drug holiday times set constant for the entirety of the simulation. Once again, we set the drug dosage to be constant for the entirety of the treatment periods. Using the parameter values from Table 2, we simulate a sample intermittent protocol with 8 time steps on therapy and 4 time steps off, arbitrarily chosen (Fig. 4). The effects of the intermittent nature of the protocol can clearly be seen reflected in the ecological, evolutionary, and demographic dynamics of the population. Before progression, during

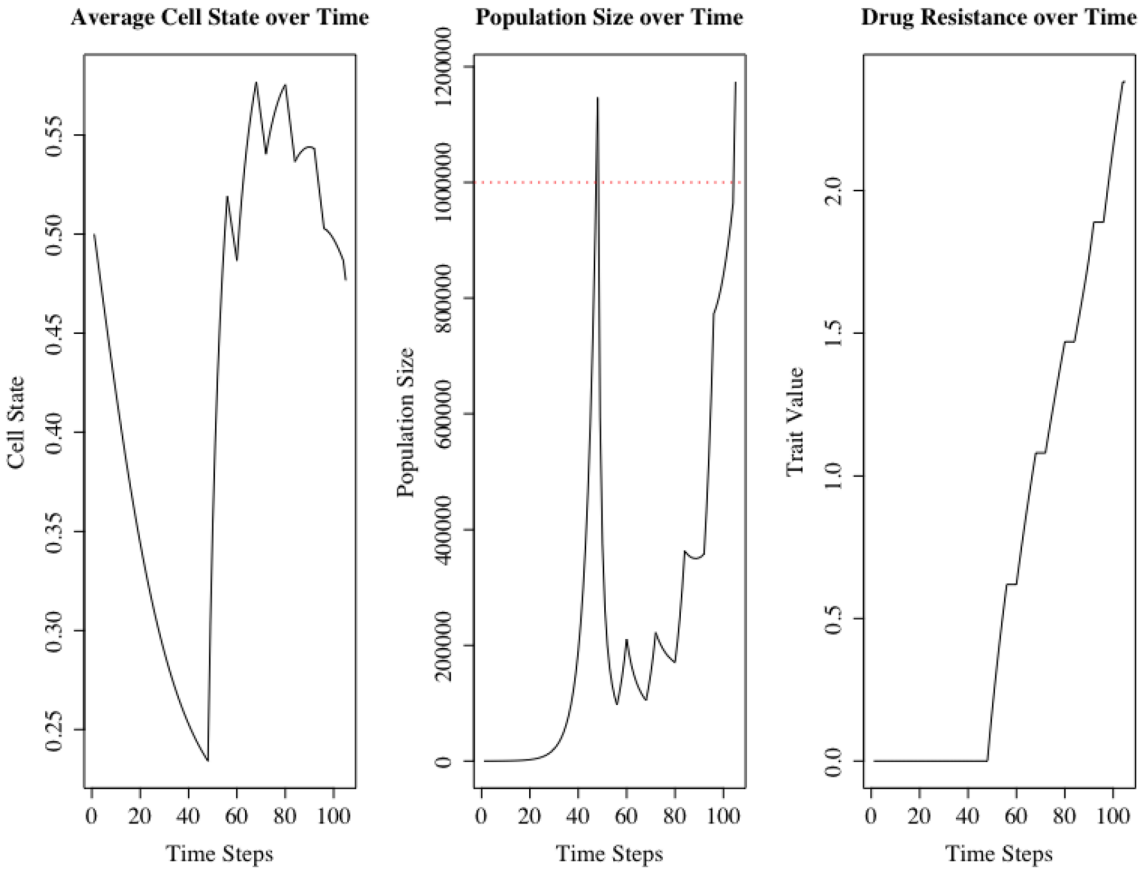

Fig. 4 Intermittent therapy protocol. Longer holidays/shorter treatment times lead to higher minima, a shorter time to progression, but a longer time to treatment failure

periods of therapy, the population size decreases, resistance evolves, and the population shifts toward lower cell states. As cells gain resistance, however, each of these trends becomes less severe. Once progression occurs, the population is able to proliferate and reduce their cell state even in the presence of therapy (albeit in a less effective manner).

To better understand the effects of intermittent therapy, we simulate a range of treatment times and drug holidays and summarize key statistics in Fig. 5. Greater drug holiday durations and lower treatment times lead to higher minima as the therapy is not given enough time to reduce the population down to its minimum. Longer holidays and shorter treatment durations also lead to shorter TTP (since the population recovers to higher levels) and a longer TTF (since resistance evolves less quickly). Thus, assuming no cost of resistance, continuous therapy is more effective for extinction and control purposes when only one drug is available. On the other hand, including drug holidays may be more effective for multi-drug control.

Next, we turn to our adaptive therapy protocol. Under this protocol, we administer therapy when the population increases past a threshold and remove therapy when the population decreases below another threshold. We first create a sample adaptive therapy protocol by setting the upper threshold to 800,000 cells and the lower threshold to 400,000 cells, arbitrarily chosen (Fig. 6). As before, we can clearly see the impacts of treatment times and treatment holidays on the eco-evo-demo dynamics of the population. Due to the adaptive nature of the dosing, we note that switching treatment on and off is more frequent at the beginning of therapy, when cells are relatively more sensitive to the drug. As cells gain resistance, therapy must be given for longer periods of time to push the population below the lower threshold. As before, drug dosage is held constant during treatment periods.

To gain a deeper understanding on how the thresholds we set impact TTP and TTF, we simulate adaptive therapy protocols over a range of thresholds (Fig. 7). As we can see, higher thresholds for starting and stopping therapy lead to a shorter TTP and a longer TTF. High thresholds induce more therapy cycles than lower thresholds because less therapy is required to reduce the population down to the threshold bounds. This prolongs the time required to gain resistance; however, since the population is cycling at high levels, progression is not far once the cells escape.

Under this model formulation, we assume no cost of resistance. This leads to an infinite improvement model of evolution, in which u is monotonically increasing. While this is a valid assumption in some cases, many cancers exhibit such costs. If we instead include a cost of resistance (as exists in many cancers (Gallaher et al. 2018; Jensen et al. 2015; Kam et al. 2015; Smalley et al. 2019)), we expect u to decrease during times of drug holidays and become re-sensitized, at least to some degree, to therapy upon the next administration. This could conceivably prolong TTP and TTF and may change our qualitative observations.

To test this hypothesis, we let $b(u,z) = b_1 exp(b_2 z + b_3 u)$ where $b_3 = -0.2$. This induces a proliferation-resistance trade-off. For biological realism, we force $u \geq 0$ to prevent negative resistance values pre-therapy. Using a drug dosage of $m = 0.7$, we simulate continuous therapy, intermittent therapy, and adaptive therapy protocols (Fig. 8). For intermittent therapy, therapy is on for 8 time steps, then turned off for 4 time steps. For adaptive therapy, we use an upper threshold of 800,000 cells and a lower bound of 400,000 cells.

Due to the cost of resistance, during times of therapy, u increases, but during times of drug holiday, u decreases, leading to resensitization of therapy. In all cases, this leads to lower overall levels of resistance and prolongs TTF and TTP (Table 4). However, even with this cost, we notice the same general trends as before: Continuous therapy is more effective at producing a low minimum of the population and promotes the longest TTP. On the other hand, intermittent and adaptive therapies are effective at keeping resistance levels low in the population, promoting a longer TTF.

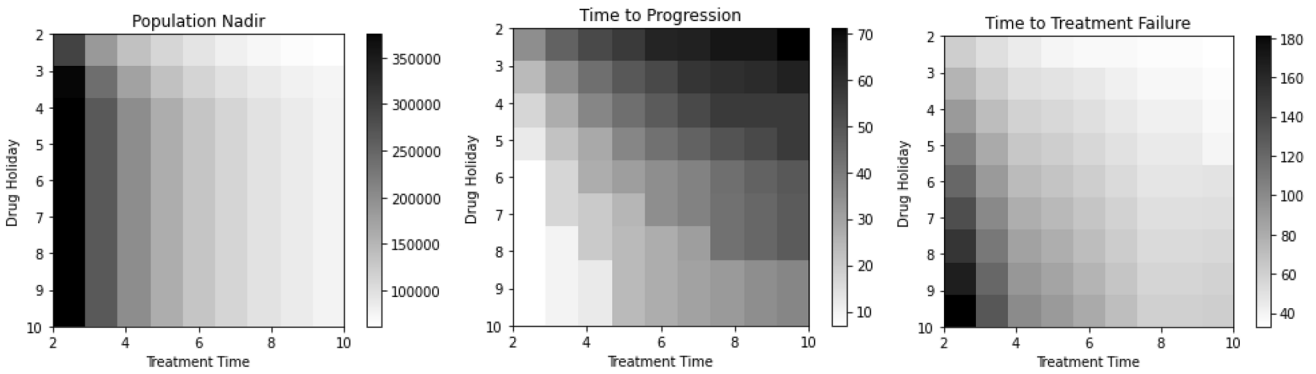

Fig. 5 Intermittent therapy: minimum of population, time to progression, and time to failure

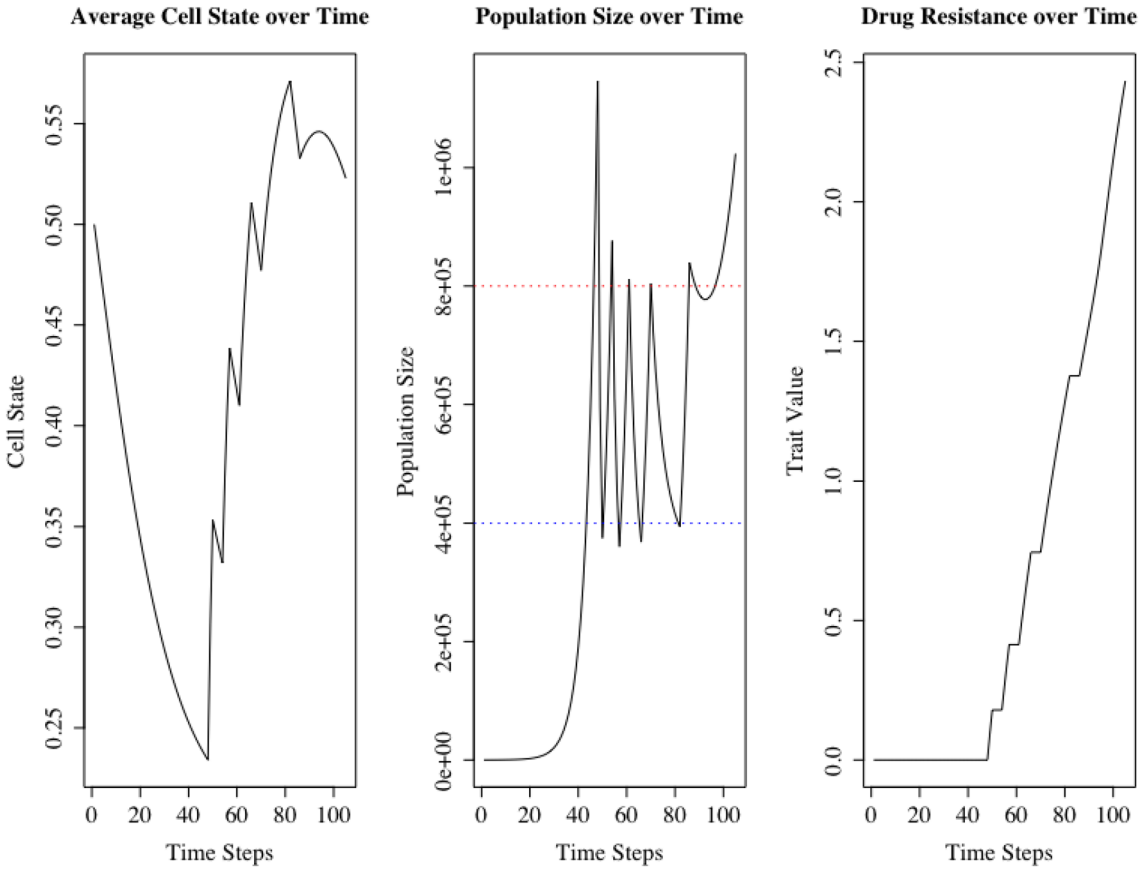

Fig. 6 Adaptive therapy protocol. Higher thresholds for starting and stopping therapy leads to a shorter time to progression and a longer time to treatment failure

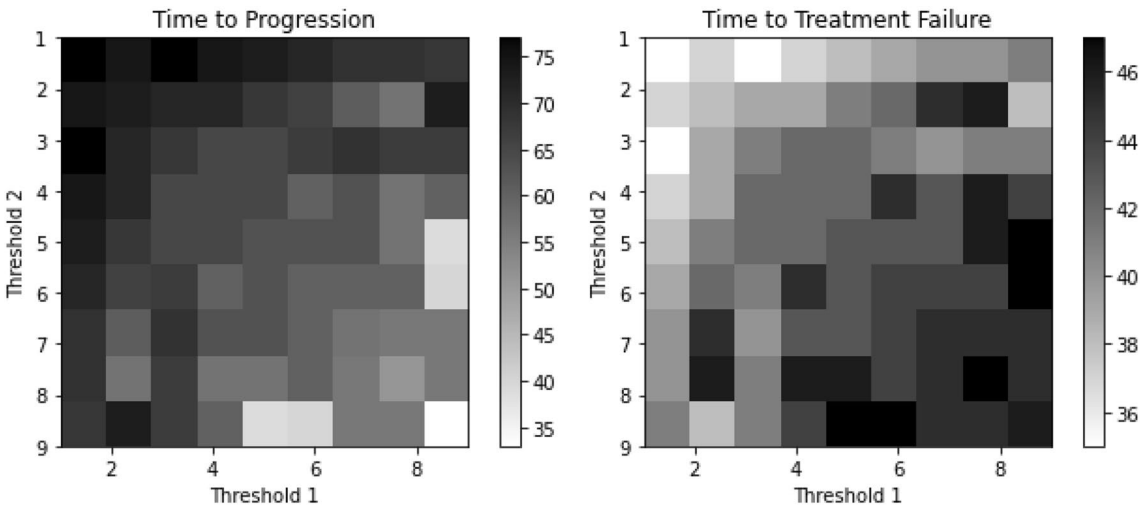

Fig. 7 Impact of thresholds on adaptive therapy protocols: time to progression and time to failure

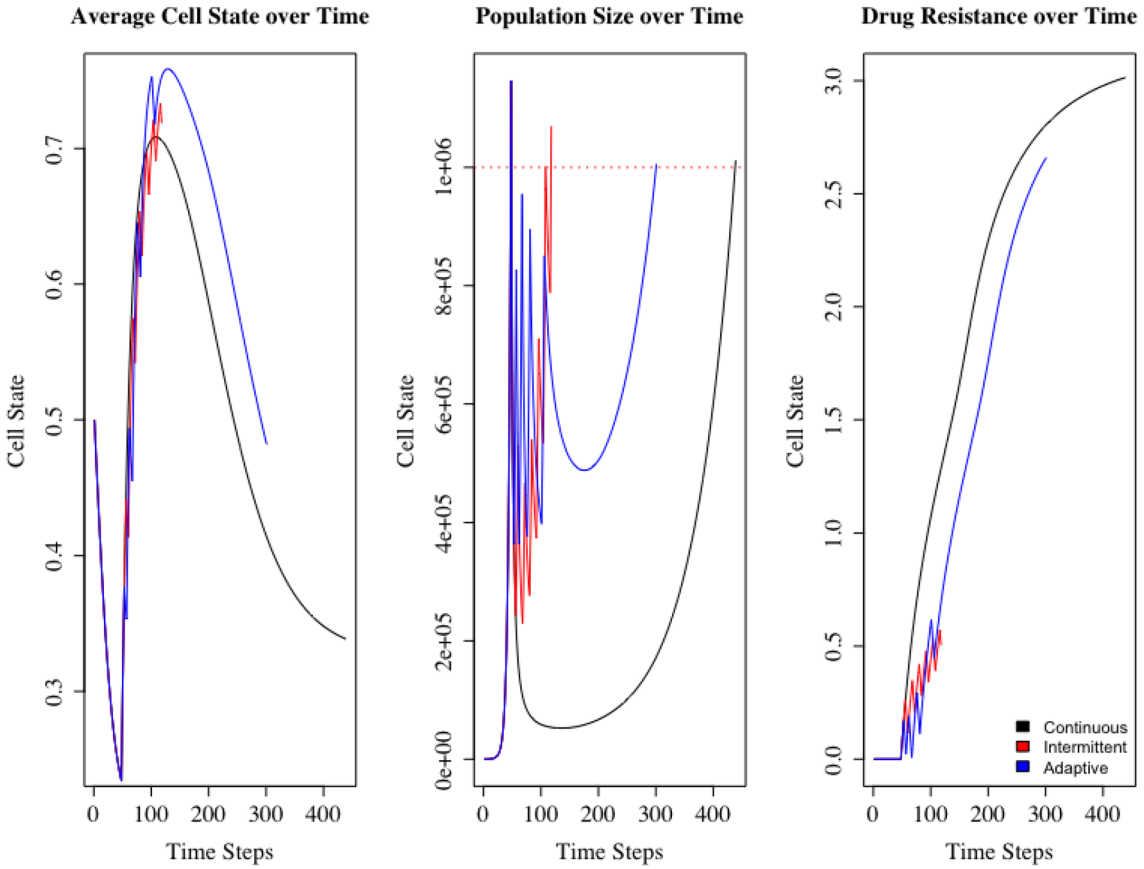

Fig. 8 Impact of cost of resistance on continuous, intermittent, and adaptive therapy protocols. The cost of resistance leads to higher times to progression and failure and lower resistance levels across the board. However, the same qualitative trends hold, with continuous therapy leading to a lower population minimum and higher time to progression, whereas intermittent and adaptive therapies lead to higher times to failure

Table 4 Continuous, intermittent, and adaptive therapy with cost of resistance summary

	Continuous therapy	Intermittent therapy	Adaptive therapy
Drug resistance	3.014	0.504	2.660
Minimum of population	52,585	228,928	488,300
Time to progression	391	70	253

Conclusion

In this paper, we developed a novel theoretical framework using IPMs to examine stress-induced responses in bacterial and cancer cell populations. This framework allowed us to simultaneously consider the roles of plasticity (in a continuous, rather than discrete sense) and gradual genetic evolution in a population's ability to respond to stressful environments. Currently, few methods exist to model both mutationally driven resistance and plasticity apart from our prior work on matrix population modeling (Bukkuri and Brown 2023; Bukkuri et al. 2022a; Bukkuri et al. 2022b). The key contribution of this paper is to add to this literature of modeling tools for eco-evo-demo dynamics. We found that faster evolving (i.e., highly evolvable) and more plastic populations (i.e., those with a high growth variance) are able to respond to stress effectively, avoiding extinction and causing treatment failure and progression rapidly. The interplay between plasticity and evolvability is a complex and practically relevant one: faster evolving species shift cell states less dramatically, and highly plastic populations evolve less mutationally-driven resistance. This observation may have implications for therapeutic regimens aimed at long-term control and life-history enlightened strategies (Bukkuri et al. 2022a). We branched into facultative stress-induced responses, in which plasticity and evolvability were condition-dependent. We found

that these mechanisms were even more effective at promoting evolutionary rescue in the population and led to faster proliferation pre-therapy, higher minima, and shorter times to progression and treatment failure. We then considered intermittent and adaptive therapy regimens. Although continuous therapy is generally more effective if the goal is extinction or control with a single drug, introducing drug holidays can prolong TTF, an important aspect if the goal is multi-drug control.

Our study has several limitations. Being theoretical in nature, our parameter values were not informed by data. Future work could seek to calibrate and compare models with time-series RNA sequencing (at bulk or single-cell resolution) and population count data pre-therapy, during therapy, and after therapy. Furthermore, complementary methods such as agent-based modeling techniques could be employed for finer resolution and stochasticity. Different forms of the cost of evolvability and resistance, biased kernels for adaptive mutations and directed plastic transitions, and density dependence are all things future work can consider.

Theoretically, we hope to expand our modeling framework to include several continuous states. For instance, we could model the stochastic reversal of evolutionary resistance (a plausible outcome when a resistant population is left without therapy for extended periods of time) by treating resistance as a second state. We also hope to include hybrid discrete and continuous states, a notion particularly important when incorporating a polyploid state (Bukkuri et al. 2022b; Bukkuri et al. 2022a) or considering primary and metastatic tumors or habitat heterogeneity within a tumor (Cunningham et al. 2021). Finally, we hope that future work will apply this framework to the specific problems mentioned here: the epithelial-to-mesenchymal transition, ADRN–MES transition in neuroblastoma, and the PAT transition, as well as additional biological conundrums such as the stem-cell paradigm in wound healing and macrophage polarization.

Supplementary Information The online version contains supplementary material available at https://doi.org/10.1007/s12064-023-00410-3.

Acknowledgements The author would like to thank Stina Andersson, Joel S. Brown, and Sofie Mohlin for valuable conversations related to this project.

Funding AB acknowledges support by the Stiftelsen Längmanska kulturfonden (BA22-0753), the Royal Swedish Academy of Sciences Stiftelsen GS Magnusons fond (MG2022-0019), the Crafoord foundation (20220633), and the National Science Foundation Graduate Research Fellowship Program (Grant No. 1746051).

Data availability Codes used to produce plots in this paper can be found at https://github.com/abukkuri/IPM_StressResponses.

Declarations

Conflict of interest On behalf of all authors, the corresponding author states that there is no conflict of interest.

References

Adler PB, Ellner SP, Levine JM (2010) Coexistence of perennial plants: an embarrassment of niches. Ecol Lett 13(8):1019–1029

Sánchez-Danés A, Larsimont JC, Liagre M, Muñoz-Couselo E, Lapouge G, Brisebarre A, Dubois C, Suppa M, Sukumaran V, del Marmol V, Tabernero J, Blanpain C (2018) A slow-cycling LGR5 tumour population mediates basal cell carcinoma relapse after therapy. Nature 562(7727):434–438

Aiello NM, Maddipati R, Norgard RJ, Balli D, Li J, Yuan S, Yamazoe T, Black T, Sahmoud A, Furth EE, Bar-Sagi D, Stanger BZ (2018) EMT subtype influences epithelial plasticity and mode of cell migration. Dev Cell 45(6):681–695

Amend SR, Torga G, Lin KC, Kostecka LG, De Marzo A, Austin RH, Pienta KJ (2019) Polyploid giant cancer cells: unrecognized actuators of tumorigenesis, metastasis, and resistance. Prostate 79(13):1489–1497

Bukkuri A, Pienta KJ, Austin RH, Hammarlund EU, Amend SR, Brown JS (2022) A life history model of the ecological and evolutionary dynamics of polyaneuploid cancer cells. Sci Rep 12(1):13713

Bukkuri A, Brown JS (2021) Evolutionary game theory: Darwinian dynamics and the G function approach. MDPI Games 12(4):1–19

Bukkuri A, Brown JS (2023) Integrating eco-evolutionary dynamics into matrix population models for structured populations: discrete and continuous frameworks. Methods Ecol Evol. https://doi.org/10.1111/2041-210X.14111

Badyaev AV (2005) Stress-induced variation in evolution: from behavioural plasticity to genetic assimilation. Pro R Soc B Biol Sci 272(1566):877–886

Basener WF, Sanford JC (2018) The fundamental theorem of natural selection with mutations. J Math Biol 76(7):1589–1622

Biehs B, Dijkgraaf GJ, Piskol R, Alicke B, Boumahdi S, Peale F, Gould SE, de Sauvage FJ (2018) A cell identity switch allows residual bcc to survive hedgehog pathway inhibition. Nature 562(7727):429–433

Zaman SB, Hussain MA, Nye R, Mehta V, Mamun KT, Hossain N (2017) A review on antibiotic resistance: alarm bells are ringing. Cureus. https://doi.org/10.7759/cureus.1403

Boshuizen J, Koopman LA, Krijgsman O, Shahrabi A, Heuvel, van den EG, Ligtenberg MA, Vredevoogd DW, Kemper K, Kuilman T, Song JY, Pencheva N, Mortensen JT, Foppen MG, Rozeman EA, Blank CU, Janmaat ML, Satijn D, Breij ECW, Peeper DS, Parren PWHI, (2018) Cooperative targeting of melanoma heterogeneity with an AXL antibody-drug conjugate and BRAF/MEK inhibitors. Nat Med 24(2):203–212

Bukkuri A, Pienta KJ, Amend SR, Hammarlund EU, Brown JS (2022) The contribution of evolvability to the eco-evolutionary dynamics of competing species. Ecol Evol 13(10):e10591

Bukkuri A, Pienta KJ, Austin RH, Hammarlund EU, Amend SR, Brown JS (2022) Stochastic models of Mendelian and reverse transcriptional inheritance in state-structured cancer populations. Sci Rep 12(1):13079

Caswell H (2001) Matrix population models: construction, analysis, and interpretation. Sinauer associates

Coulson T (2012) Integral projections models, their construction and use in posing hypotheses in ecology. Oikos 121(9):1337–1350

Coulson T, Tuljapurkar S, Childs DZ (2010) Using evolutionary demography to link life history theory, quantitative genetics and population ecology. J Anim Ecol 79(6):1226–1240

Cunningham JJ, Bukkuri A, Gatenby RA, Brown JS, Gillies RJ (2021) Coupled source-sink habitats produce spatial and temporal variation of cancer cell molecular properties as an alternative to branched clonal evolution and stem cell paradigms. Front Ecol Evol 9:472

Dahlgren JP, Ehrlén J (2009) Linking environmental variation to population dynamics of a forest herb. J Ecol 97(4):666–674

Dalgleish HJ, Koons DN, Hooten MB, Moffet CA, Adler PB (2011) Climate influences the demography of three dominant sagebrush steppe plants. Ecology 92(1):75–85

de Vries C, Desharnais RA, Caswell H (2020) A matrix model for density-dependent selection in stage-classified populations, with application to pesticide resistance in Tribolium. Ecol Model 416:1

Dhawan A, Madani Tonekaboni SA, Taube JH, Hu S, Sphyris N, Mani SA, Kohandel M (2016) Mathematical modelling of phenotypic plasticity and conversion to a stem-cell state under hypoxia. Sci Rep 6:1–10

Diamond SE, Martin RA (2016) The interplay between plasticity and evolution in response to human-induced environmental change. F1000 Res 5:2835

Diekmann O (2004) A beginner's guide to adaptive dynamics. Math Model Popul Dyn 63:47–86

Guler GD, Tindell CA, Pitti R, Wilson C, Nichols K, Cheung TKW, Kim HJ, Wongchenko M, Yan Y, Haley B, Cuellar T, Webster J, Alag N, Hegde G, Jackson E, Nance TL, Giresi PG, Chen KB, Liu J, Jhunjhunwala S, Settleman J, Stephan JP, Arnott D, Classon M (2017) Repression of stress-induced LINE-1 expression protects cancer cell subpopulations from lethal drug exposure. Cancer Cell 32(2):221–237

Hanahan D, Weinberg RA (2011) Hallmarks of cancer: the next generation. Cell 144(5):646–674

Easterling MR, Ellner SP, Dixon PM (2000) Size-specific sensitivity: applying a new structured population model. Ecology 81(3):694–708

Ellner SP, Rees M (2006) Integral projection models for species with complex demography. Am Nat 167(3):410–428

Hesse E, Rees M, Müller-Schärer H (2008) Life-history variation in contrasting habitats: flowering decisions in a clonal perennial herb (Veratrum album). Am Nat 172(5):E196

Erickson RA, Eager EA, Kocovsky PM, Glover DC, Kallis JL, Long KR (2018) A spatially discrete, integral projection model and its application to invasive carp. Ecol Model 387(163–171):11

Kisdi É, Stefan A, Geritz H (2010) Adaptive dynamics: a framework to model evolution in the ecological theatre. J Math Biol 61(1):165

Finch CE, Goodman MF (1997) Relevance of "adaptive" mutations arising in non-dividing cells of microorganisms to age-related changes in mutant phenotypes of neurons. Trends Neurosci 20(11):501–507

Fisher RA, Gollan B, Helaine S (2017) Persistent bacterial infections and persister cells. Nat Rev Microbiol 15(8):453–464

Fitzgerald DM, Hastings PJ, Rosenberg SM (2017) Implications in cancer and drug resistance. stress-induced mutagenesis. Annu Rev Cancer Biol 1:119–140

Nicolè F, Dahlgren JP, Vivat A, Till-Bottraud I, Ehrlén J (2011) Interdependent effects of habitat quality and climate on population growth of an endangered plant. J Ecol 99(5):1211–1218

Forouzannia F, Sivaloganathan S, Kohandel M (2020) A mathematical study of the impact of cell plasticity on tumour control probability. Mathematical Biosciences and Engineering 17(5):5250–5266

Foster PL (2007) Stress-induced mutagenesis in bacteria. Crit Rev Biochem Mol Biol 42(5):373–397

Fox RJ, Donelson JM, Schunter C, Ravasi T, Gaitán-Espitia JD (2019) Beyond buying time: the role of plasticity in phenotypic adaptation to rapid environmental change. Philos Trans R Soc B Biol Sci 374(1768):20180174

Frank SA, Slatkin M (1992) Fisher's fundamental theorem of natural selection. Trends Ecol Evol 7(3):92–95

Galhardo RS, Do R, Yamada M, Friedberg EC, Hastings PJ, Nohmi T, Rosenberg SM (2009) DinB upregulation is the sole role of the SOS response in stress-induced mutagenesis in Escherichia coli. Genetics 182(1):55–68

Gallaher JA, Enriquez-Navas PM, Luddy KA, Gatenby RA, Anderson ARA (2018) Spatial heterogeneity and evolutionary dynamics modulate time to recurrence in continuous and adaptive cancer therapies. Cancer Res 78(8):2127–2139

Gatenby RA, Silva AS, Gillies RJ, Frieden BR (2009) Adaptive therapy. Cancer Res 69(11):4894–4903

Housman G, Byler S, Heerboth S, Lapinska K, Longacre M, Snyder N, Sarkar S (2014) Drug resistance in cancer: an overview. Cancers 6(3):1769

Goldschmidt R (1933) Some aspects of evolution. Science 78(2033):539–547

Goodsman DW, Aukema BH, McDowell NG, Middleton RS, Xu C (2018) Incorporating variability in simulations of seasonally forced phenology using integral projection models. Ecol Evol 8(1):162–175

Caswell H (2012) Matrix models and sensitivity analysis of populations classified by age and stage: a vec-permutation matrix approach. Theor Ecol 5(3):403–417

Caswell H (2019) Sensitivity analysis: matrix methods in demography and ecology. Demographic research monographs. Springer International Publishing, Cham

Hall BG (1995) Adaptive mutations in Escherichia coli as a model for the multiple mutational origins of tumors. Proc Nat Acad Sci USA 92(12):5669–5673

Hangauer MJ, Viswanathan VS, Ryan MJ, Bole D, Eaton JK, Matov A, Galeas J, Dhruv HD, Berens ME, Schreiber SL, McCormick F, McManus MT (2017) Drug-tolerant persister cancer cells are vulnerable to GPX4 inhibition. Nature 551(7679):247–250

Hastings PJ, Slack A, Petrosino JF, Rosenberg SM (2004) Adaptive amplification and point mutation are independent mechanisms: evidence for various stress-inducible mutation mechanisms. PLoS Biol 2(12):e399

Gonzalez H, Mei W, Robles I, Hagerling C, Allen BM, Okholm TLH, Nanjaraj A, Verbeek T, Kalavacherla S, Gogh, van M, Georgiou S, Daras M, Phillips JJ, Spitzer MH, Roose JP, Werb Z (2022) Cellular architecture of human brain metastases. Cell. https://doi.org/10.1101/2023.07.03.547523

Smalley I, Kim E, Li J, Spence P, Wyatt CJ, Eroglu Z, Sondak VK, Messina JL, Babacan NA, Maria-Engler SS, De Armas L, Williams SL, Gatenby RA, Ann Chen Y, Anderson ARA, Smalley KSM (2019) Leveraging transcriptional dynamics to improve BRAF inhibitor responses in melanoma. EBioMedicine 48:178

Bjedov I, Tenaillon O, Gérard B, Souza V, Denamur E, Radman M, Taddei F, Matic I (2003) Stress-induced mutagenesis in bacteria. Science 300(5624):373–397

Tsoi J, Robert L, Paraiso K, Galvan C, Sheu KM, Lay J, Wong DJ, Atefi M, Shirazi R, Wang X, Braas D, Grasso CS, Palaskas N, Ribas A, Graeber TG (2018) Multi-stage differentiation defines melanoma subtypes with differential vulnerability to drug-induced iron-dependent oxidative stress. Cancer Cell 33(5):890–904

Jensen NF, Stenvang J, Beck MK, Hanáková B, Belling KC, Do KN, Viuff B, Nygård SB, Gupta R, Rasmussen MH, Tarpgaard LS, Hansen TP, Budinská E, Pfeiffer P, Bosman F, Tejpar S, Roth A, Delorenzi M, Andersen CL, Rømer MU, Brünner N, Moreira JMA (2015) Establishment and characterization of models of chemotherapy resistance in colorectal cancer:

towards a predictive signature of chemoresistance. Mol Oncol 9(6):1169–1185
Metcalf CJE, Graham AL, Martinez-Bakker M, Childs DZ (2016) Opportunities and challenges of integral projection models for modelling host-parasite dynamics. J Anim Ecol 85(2):343–355
Hegland SJ, Jongejans E, Rydgren K (2010) Investigating the interaction between ungulate grazing and resource effects on Vaccinium myrtillus populations with integral projection models. Oecologia 163(3):695–706
Zañudo JGT, Guinn MT, Farquhar K, Szenk M, Steinway SN, Balázsi G, Albert R (2019) Towards control of cellular decision-making networks in the epithelial-to-mesenchymal transition. Phys Biol 16(3):031002
Merilä J, Hendry AP (2014) Climate change, adaptation, and phenotypic plasticity: the problem and the evidence. Evol Appl 7(1):1–14
Kam Y, Das T, Tian H, Foroutan P, Ruiz E, Martinez G, Minton S, Gillies RJ, Gatenby RA (2015) Sweat but no gain: inhibiting proliferation of multidrug resistant cancer cells with ersatzdroges. Int J Cancer 136(4):E188–E196
Katsuno Y, Meyer DS, Zhang Z, Shokat KM, Akhurst RJ, Miyazono K, Derynck R (2019) Chronic TGF-β exposure drives stabilized EMT, tumor stemness, and cancer drug resistance with vulnerability to bitopic mTOR inhibition. Sci Signal 12(570):eaau8544
Wallner L, Dai J, Escara-Wilke J, Zhang J, Yao Z, Lu Y, Trikha M, Nemeth JA, Zaki MH, Keller ET (2006) Inhibition of interleukin-6 with CNTO328, an anti-interleukin-6 monoclonal antibody, inhibits conversion of androgen-dependent prostate cancer to an androgen-independent phenotype in orchiectomized mice. Cancer Res 66(6):3087–3095
Layton JC, Foster PL (2003) Error-prone DNA polymerase IV is controlled by the stress-response sigma factor, RpoS. E. coli. Mol Microbiol 50(2):549–561
Lessard S (1997) Fisher's fundamental theorem of natural selection revisited. Theor Popul Biol 52(2):119–136
Chin VL, Lim CL (2019) Epithelial-mesenchymal plasticity - engaging stemness in an interplay of phenotypes. Stem Cell Investig 6:25
Li CC (1967) Fundamental theorem of natural selection. Nature 214(5087):4
Liau BB, Sievers C, Donohue LK, Gillespie SM, Flavahan WA, Miller TE, Venteicher AS, Hebert CH, Carey CD, Rodig SJ, Shareef SJ, Najm FJ, van Galen P, Wakimoto H, Cahill DP, Rich JN, Aster JC, Suvà ML, Patel AP, Bernstein BE, (2017) Adaptive chromatin remodeling drives glioblastoma stem cell plasticity and drug tolerance. Cell Stem Cell 20(2):233–246
Li S, Song Y, Quach C, Guo H, Jang GB, Maazi H, Zhao S, Sands NA, Liu Q, In Gino K, Peng D, Yuan W, Machida K, Yu M, Akbari O, Hagiya A, Yang Y, Punj V, Tang L, Liang C (2019) Transcriptional regulation of autophagy-lysosomal function in BRAF-driven melanoma progression and chemoresistance. Nat Commun 10(1):1693
Lombardo MJ, Aponyi I, Rosenberg SM (2004) General stress response regulator RpoS in adaptive mutation and amplification in Escherichia coli. Genetics 166(2):669–680
Lovett ST (2006) Replication arrest-stimulated recombination: dependence on the RecA paralog, RadA/Sms and translesion polymerase. DinB DNA Repair 5(12):1421–1427
Tonekaboni SAM, Dhawan A, Kohandel M (2017) Mathematical modelling of plasticity and phenotype switching in cancer cell populations. Math Biosci 283:30–37
Frieri M, Kumar K, Boutin A (2017) Antibiotic resistance. J Infect Pub Health 10(4):369–378
Rabé M, Dumont S, Álvarez-Arenas A, Janati H, Belmonte-Beitia J, Calvo GF, Thibault-Carpentier C, Séry Q, Chauvin C, Joalland N, Briand F, Blandin S, Scotet E, Pecqueur C, Clairambault J, Oliver L, Perez-Garcia V, Nadaradjane A, Cartron PF, Gratas C, Vallette FM (2020) Identification of a transient state during the acquisition of temozolomide resistance in glioblastoma. Cell Death Dis 11(1):19
Merow C, Dahlgren JP, Metcalf CJE, Childs DZ, Evans MEK, Jongejans E, Record S, Rees M, Salguero-Gómez R, Mcmahon SM (2014) Advancing population ecology with integral projection models: a practical guide. Methods Ecol Evol 5(2):99–110
Metcalf JC, Rose KE, Rees M (2003) Evolutionary demography of monocarpic perennials. Trends Ecol Evol 18(9):471–480
Dietrich MR (2003) Richard Goldschmidt: hopeful monsters and other 'heresies'
Miller TEX, Louda SM, Rose KA, Eckberg JO (2009) Impacts of insect herbivory on cactus population dynamics: Experimental demography across an environmental gradient. Ecol Monogr 79(1):155–172
Miller TEX, Williams JL, Jongejans E, Brys R, Jacquemyn H (2012) Evolutionary demography of iteroparous plants: incorporating non-lethal costs of reproduction into integral projection models. Proc R Soc B Biol Sci 279(1739):2831–2840
Petrosino JF, Galhardo RS, Morales LD, Rosenberg SM (2009) Stress-induced β-lactam antibiotic resistance mutation and sequences of stationary-phase mutations in the Escherichia coli chromosome. J Bacteriol 191(19):5881–5889
Pienta KJ, Hammarlund EU, Axelrod R, Brown JS, Amend SR (2020) Poly-aneuploid cancer cells promote evolvability, generating lethal cancer. Evol Appl 13(7):1626–1634
Pienta KJ, Hammarlund EU, Hammarlund EU, Axelrod R, Amend SR, Brown JS (2020) Convergent evolution, evolving evolvability, and the origins of lethal cancer. Mol Cancer Res 18(6):801–810
Pienta KJ, Hammarlund EU, Austin RH, Axelrod R, Brown JS, Amend SR (2020) Cancer cells employ an evolutionarily conserved polyploidization program to resist therapy. Sem Cancer Biol 81:145
Pienta KJ, Hammarlund EU, Brown JS, Amend SR, Axelrod RM (2021) Cancer recurrence and lethality are enabled by enhanced survival and reversible cell cycle arrest of polyaneuploid cells. Proc Nat Acad Sci USA 118(7):2
Rambow F, Rogiers A, Marin-Bejar O, Aibar S, Femel J, Dewaele M, Karras P, Brown D, Chang YH, Debiec-Rychter M, Adriaens C, Radaelli E, Wolter P, Bechter O, Dummer R, Levesque M, Piris A, Frederick DT, Boland G, Flaherty KT, van den Oord J, Voet T, Aerts S, Lund AW, Marine JC (2018) Toward minimal residual disease-directed therapy in melanoma. Cell 174(4):843–855
Rees M, Rose KE (2002) Evolution of flowering strategies in Oenothera glazioviana: an integral projection model approach. Proc R Soc B Biol Sci 269(1499):1509–1515
Rees M, Childs DZ, Ellner SP (2014) Building integral projection models: a user's guide. J Anim Ecol 83(3):528–545
Rose KE, Louda SM, Rees M (2005) Demographic and evolutionary impacts of native and invasive insect herbivores on Cirsium canescens. Ecology 86(2):453–465
Rosenberg SM (2001) Evolving responsively: adaptive mutation. Nat Rev Genet 2(7):504–515
Rosenberg SM, Longerich S, Gee P, Harris RS (1994) Adaptive mutation by deletions in small mononucleotide repeats. Science 265(5170):405–407
Rosenberg SM, Shee C, Frisch RL, Hastings PJ (2012) Stress-induced mutation via DNA breaks in Escherichia coli : a molecular mechanism with implications for evolution and medicine. BioEssays 34(10):885–892
Roswall P, Bocci M, Bartoschek M, Li H, Kristiansen G, Jansson S, Lehn S, Sjölund J, Reid S, Larsson C, Eriksson P, Anderberg C, Cortez E, Saal LH, Orsmark-Pietras C, Cordero E, Haller BK, Häkkinen J, Burvenich IJG, Lim E, Orimo A, Höglund M, Rydén L, Moch H, Scott AM, Eriksson U, Pietras K (2018) Microenvironmental control of breast cancer subtype elicited through

paracrine platelet-derived growth factor-CC signaling. Nat Med 24(4):463–473

Rusan M, Li K, Li Y, Christensen CL, Abraham BJ, Kwiatkowski N, Buczkowski KA, Bockorny B, Chen T, Li S, Rhee K, Zhang H, Chen W, Terai H, Tavares T, Leggett AL, Li T, Wang Y, Zhang T, Kim TJ, Hong SH, Poudel-Neupane N, Silkes M, Mudianto T, Tan L, Shimamura T, Meyerson M, Bass AJ, Watanabe H, Gray NS, Young RA, Wong KK, Hammerman PS (2018) Suppression of adaptive responses to targeted cancer therapy by transcriptional repression. Cancer Discov 8(1):59–73

Schwartz LM, Gibson DJ, Young BG (2016) Using integral projection models to compare population dynamics of four closely related species. Popul Ecol 58(2):285–292

Shaffer SM, Dunagin MC, Torborg SR, Torre EA, Emert B, Krepler C, Beqiri M, Sproesser K, Brafford PA, Xiao M, Eggan E, Anastopoulos IN, Vargas-Garcia CA, Singh A, Nathanson KL, Herlyn M, Raj A (2017) Rare cell variability and drug-induced reprogramming as a mode of cancer drug resistance. Nature 546(7658):431–435

Sharma SV, Lee DY, Li B, Quinlan MP, Takahashi F, Maheswaran S, McDermott U, Azizian N, Zou L, Fischbach MA, Wong KK, Brandstetter K, Wittner B, Ramaswamy S, Classon M, Settleman J (2010) A chromatin-mediated reversible drug-tolerant state in cancer cell subpopulations. Cell 141(1):69

Shen S, Clairambault J (2020) Cell plasticity in cancer cell populations. F1000Res 9:635

Shen S, Faouzi S, Bastide A, Martineau S, Malka-Mahieu H, Fu YU, Sun X, Mateus C, Routier E, Roy S, Desaubry L, André F, Eggermont A, David A, Scoazec JY, Vagner S, Robert C (2019) An epitranscriptomic mechanism underlies selective mRNA translation remodelling in melanoma persister cells. Nat Commun 10(1):5713

Strauss BS (1986) The origin of point mutations in human tumor cells. Cancer Res 52(2):249–253

Straussman R, Morikawa T, Shee K, Barzily-Rokni M, Qian ZR, Du J, Davis A, Mongare MM, Gould J, Frederick DT, Cooper ZA, Chapman PB, Solit DB, Ribas A, Lo RS, Flaherty KT, Ogino S, Wargo JA, Golub TR (2012) Tumour micro-environment elicits innate resistance to RAF inhibitors through HGF secretion. Nature 487(7408):500–504

Vasan N, Baselga J, Hyman DM (2019) A view on drug resistance in cancer. Nature 575(7782):299–309

Vincent TL, Brown JS (2005) Evolutionary game theory, natural selection, and darwinian dynamics. Cambridge University Press

Viswanathan VS, Ryan MJ, Dhruv HD, Gill S, Eichhoff OM, Seashore-Ludlow B, Kaffenberger SD, Eaton JK, Shimada K, Aguirre AJ, Viswanathan SR, Chattopadhyay S, Tamayo P, Yang WS, Rees MG, Chen S, Boskovic ZV, Javaid S, Huang C, Wu X, Tseng YY, Roider EM, Gao D, Cleary JM, Wolpin BM, Mesirov JP, Haber DA, Engelman JA, Boehm JS, Kotz JD, Hon CS, Chen Y, Hahn WC, Levesque MP, Doench JG, Berens ME, Shamji AF, Clemons PA, Stockwell BR, Schreiber SL (2017) Dependency of a therapy-resistant state of cancer cells on a lipid peroxidase pathway. Nature 547(7664):453–457

Weng CH, Chen LY, Lin YC, Shih JY, Lin YC, Tseng RY, Chiu AC, Yeh YH, Liu C, Lin YT Fang JM, Chen CC (2019) Epithelial-mesenchymal transition (EMT) beyond EGFR mutations per se is a common mechanism for acquired resistance to EGFR TKI. Oncogene 38(4):455–468

West J, You L, Zhang J, Gatenby RA, Brown JS, Newton PK, Anderson ARA (2020) Towards multidrug adaptive therapy. Cancer Res 80(7):1578–1589

Williams JL (2009) Flowering life-history strategies differ between the native and introduced ranges of a monocarpic perennial. Am Nat 174(5):660–672

Williams JL, Auge H, Maron JL (2010) Testing hypotheses for exotic plant success: parallel experiments in the native and introduced ranges. Ecology 91(5):1355–1366

Williams JL, Miller TEX, Ellner SP, Doak DF (2012) Avoiding unintentional eviction from integral projection models. Ecology 93(9):2008–2014

Willis JC (1923) The origin of species by large, rather than by gradual, change, and by guppy's method of differentiation. Ann Bot 37(148):605–628

Yuan X, Seneviratne JA, Du S, Xu Y, Chen Y, Jin Q, Jin X, Balachandran A, Huang S, Xu Y, Zhai Y, Lu L, Tang M, Dong Y, Cheung BB, Marshall GM, Shi W, Carter DR, Zhang C (2022) Single-cell profiling of peripheral neuroblastic tumors identifies an aggressive transitional state that bridges an adrenergic-mesenchymal trajectory. Cell Rep 41(1):111455

Zhou C, Fan N, Liu F, Fang N, Plum PS, Thieme R, Gockel I, Gromnitza S, Hillmer AM, Chon SH, Schlösser HA, Bruns CJ, Zhao Y (2020) Linking cancer stem cell plasticity to therapeutic resistance-mechanism and novel therapeutic strategies in esophageal cancer. Cells 9(6):6